DC-derived IL-27 suppresses anti-tumor immunity via the modulation of gut microbiota

Yonghao Liu
Immunology Programme, Life Sciences Institute; Immunology Translational Research Program and Department of Microbiology and Immunology, Yong Loo Lin School of Medicine, National University of Singapo

Yuan Song
Immunology Programme, Life Sciences Institute; Immunology Translational Research Program and Department of Microbiology and Immunology, Yong Loo Lin School of Medicine, National University of Singapo

Huanle Gong
Institute of Blood and Marrow Transplantation, Jiangsu Institute of Hematology, The First Affiliated Hospital of Soochow University, Collaborative Innovation Center of Hematology, National Clinical R

Ziqi Jin
Center for Systems Medicine, Institute of Basic Medical Sciences, Chinese Academy of Medical Sciences & Peking Union Medical College, Beijing, China; Suzhou Institute of Systems Medicine, Suzhou, Jia

Lei Lei
Institute of Blood and Marrow Transplantation, Jiangsu Institute of Hematology, The First Affiliated Hospital of Soochow University, Collaborative Innovation Center of Hematology, National Clinical R

Ying Zhu
Immunology Programme, Life Sciences Institute; Immunology Translational Research Program and Department of Microbiology and Immunology, Yong Loo Lin School of Medicine, National University of Singapo

Yu Mei
Immunology Programme, Life Sciences Institute; Immunology Translational Research Program and Department of Microbiology and Immunology, Yong Loo Lin School of Medicine, National University of Singapo

Huey Yee Teo
Immunology Programme, Life Sciences Institute; Immunology Translational Research Program and Department of Microbiology and Immunology, Yong Loo Lin School of Medicine, National University of Singapo

Zhinan Yin
Zhuhai Precision Medical Center, Zhuhai People's Hospital (Zhuhai Hospital Affiliated with Jinan University), Jinan University, Zhuhai, China

Depei Wu
Institute of Blood and Marrow Transplantation, Jiangsu Institute of Hematology, The First Affiliated Hospital of Soochow University, Collaborative Innovation Center of Hematology, National Clinical R
Haiyan Liu (micliuh@nus.edu.sg)
Immunology Programme, Life Sciences Institute; Immunology Translational Research Program and Department of Microbiology and Immunology, Yong Loo Lin School of Medicine, National University of Singapo

---

Research Article

Keywords: IL-27p28, T cells, anti-tumor immunity, TIP-DCs, gut microbiota

Posted Date: March 17th, 2022

DOI: https://doi.org/10.21203/rs.3.rs-1452354/v1

Abstract

Background

Chronic inflammation has been shown to be crucial in promoting tumor initiation and development in many cancer types, including hepatocellular carcinoma (HCC). It is characterized by the persistent expression of inflammatory cytokines surrounding the tissues. IL-27 is a heterodimeric cytokine that consists of EBI3 and p28, which can be expressed by many antigen presenting cells, including monocytes, macrophages, and dendritic cells (DCs). The role of IL-27 in tumor development is controversial. Gut microbiota plays an important role in immune system development and homeostasis, while how it can be regulated to impact anti-tumor immune response is poorly understood.

Results

We demonstrated a tumor-promoting role of DC-derived IL-27 via the modulation of gut microbiota in murine models. IL-27p28 DC-conditional knockout (Itgax-IL-27p28$^{f/f}$) mice exhibited reduced tumor growth compared with WT controls. T cell anti-tumor response was enhanced, and inhibitory receptor expression was decreased. Interestingly, when WT mice received fecal transplant from Itgax-IL-27p28$^{f/f}$ mice, tumor growth was significantly inhibited. Their gut microbiota exhibited distinct features and gavage of bifidobacterium, a bacteria strain that was greatly increased in Itgax-IL-27p28$^{f/f}$ mice, reduced tumor growth. Furthermore, MHC class II expression on tumor necrosis factor and inducible nitric-oxide-synthase-producing DCs (TIP-DCs) was increased in Itgax-IL-27p28$^{f/f}$ mice, and their activation could be inhibited by the gut microbiota modulated by IL-27. Their function of activating CD8^{+} T cells was also enhanced in the absence of DC-derived IL-27.

Conclusion

DC-derived IL-27 could promote tumor development and suppress anti-tumor immune response by inhibiting the function of TIP-DCs via the modulation of gut microbiota. This indirect effect of IL-27 on adaptive immune response provides insights into possible organ-specific functions of IL-27 and targeting IL-27 in tumor immunotherapy.

Background

Tumor development is considered as an evolution of complex interactions between the tissue/tumor cells and tumor microenvironment[1]. Many factors affect tumor initiation and development, such as aging, cancer-inducing substances, infectious agents, radiation and diet[2]. Chronic inflammation has been shown to be crucial in promoting tumor initiation and development in many cancer types, including HCC[3]. It is characterized by the persistent expression of inflammatory cytokines surrounding the tissues. The expression and signaling dysregulation of IL-6 family cytokines, consisted of IL-6, IL-11, IL-31, ciliary neurotrophic factor (CNTF), cardiotrophin1 (CT1) and cardiotrophin-like cytokine factor 1(CLCF1),

leukemia inhibitory factor (LIF) and oncostatin M[4], in the tumor microenvironment were frequently associated with cancer progression and poor clinical outcomes[5–9]. On the other hand, IL-12 is considered as one of the most potent cytokines in mediating anti-tumor responses[10] by inducing Th1 responses and enhancing IFN-γ production, as well as promoting NK function. IL-27 was initially discovered as a member of IL-12 family[11], and later regarded as a member of IL-6 family by phylogenetic analysis[12]. Its function in tumor progression and anti-tumor immune response is still not clear.

IL-27 is a heterodimeric cytokine that consists of EBI3 and p28, which can be expressed by many antigen presenting cells, including monocytes, macrophages and DCs[11]. By binding to WSX-1 and gp130, IL-27 transduces intracellular signaling via STAT1 and STAT3 activation[13]. IL-27 was initially shown to be a pro-inflammatory cytokine that could promote Th1 responses by activating naïve $CD4^+$ T cells and NK cells to produce IFN-γ[13–15]. The pro-inflammatory function of IL-27 was later challenged by evidence that IL-27 signaling could be critical in regulating pro-inflammatory cytokine production and suppressing T cell hyperactivity during infections[16,17]. Subsequently, many studies have demonstrated the anti-inflammatory functions of IL-27 in various animal models, such as Toxoplasma gondii infection, experimental autoimmune encephalomyelitis (EAE), and chronic inflammatory bowel disease (IBD)[18–20]. Furthermore, IL-27 is also found to promote the expression of inhibitory receptors on T cells, such as Tim-3, LAG-3, and PD-1[21–23], indicating a possible mechanism for its immune suppressive function.

The role of IL-27 in tumor development is controversial. IL-27 has been shown to promote anti-tumor immune response by enhancing Th1 and CTL responses in TBJ neuroblastoma and colon carcinoma[24,25]. Other studies also indicate that IL-27 could promote NK or NKT cell activation, which results in reduced tumor growth[26,27]. However, IL-27 signaling could drive Tim-3 and IL-10 expression and T cell dysfunction in B16 melanoma[28]. Moreover, IL-27 is shown to confer a pro-tumorigenic activity by suppressing T cell function via CD39[23]. Therefore, the function of IL-27 in anti-tumor immune response is still not clear and need further investigation.

The gut microbiota plays an important role in immune system development[29,30] and homeostasis[31,32]. It has been shown that maternal microbiota could shape early postnatal innate immune development[33]. The lack of Bifidobacterium is associated with systemic and intestinal inflammation and immune dysregulation during the first months of life[34]. Many studies have demonstrated the link between gut microbiota and tumor development[35]. Studies using germ-free animals revealed tumor-promoting effects of the microbiota in variant cancers, including colorectal cancer[36] and gastric cancer[37]. Similar conclusion was made by using antibiotics that deplete intestinal microbiota[38,39]. Anti-tumor effects of some commensal bacteria strains have also been suggested. Commensal Bifidobacterium could promote anti-tumor immune responses and facilitate anti-PD-L1 treatment efficacy in murine B16 melanoma model[40]. The immune modulatory function of gut microbiota during anti-PD1 therapy was also confirmed in human melanoma patients[41]. The role of microbiota in tumor development and therapy has been studied in many tumor types, such as sarcomas, non-small cell lung cancer, renal cell carcinoma and

lymphoma[42–44]. Due to the anatomical and functional relationship between liver and gut, gut microbiota has been suggested to impact HCC development[45,46]. It has been shown that fecal microbial diversity is increased in early HCC patients[47], and patients with primary HCC exhibit increased proteobacteria, a pro-inflammatory bacteria strain, in their fecal microbiota[48]. Nevertheless, how gut microbiota can be regulated and how it can impact anti-tumor immune response are poorly understood.

DC-derived IL-27 is especially important in regulating anti-tumor immune response as DCs are essential in modulating adaptive immunity. In this study, we investigated the role of DC-derived IL-27p28 in tumor development in murine HCC models by using Itgax-IL-27p28$^{f/f}$ mice. We found that tumor development was significantly reduced in the Itgax-IL-27p28$^{f/f}$ mice and Th1/CTL responses were promoted in the absence of DC-derived IL-27p28. This enhanced anti-tumor response was dependent on both $CD4^+$ and $CD8^+$ T cells. Moreover, DC-derived IL-27 may modulate gut microbiota to affect the anti-tumor adaptive immune responses. Further studies showed that the activation of TIP-DCs could be inhibited by the gut microbiota modulated by IL-27, which resulted in suppressed T cell proliferation and function. Our results demonstrated the role of DC-derived IL-27p28 in tumor development and its function in regulating adaptive immune response via modulating gut microbiota.

Materials And Methods

Cell line

The murine HCC cell line hepa1-6 was obtained from the American Type Culture Collection (Manassas, VA) and cultured in DMEM with 10% fetal bovine serum (Gibco, Gaithersburg, MD). The murine HCC cell line hepa1-6 has recently been authenticated by mouse cell line authentication service provided by Applied Biological Materials (Richmond, BC, Canada).

Mice and murine HCC models

C57BL/6 Itgax-IL-27p28f/f mice and C57BL/6-Tg(TcraTcrb)1100Mjb/J (OT-I mice) were provided by Dr. Zhinan Yin (Jinan University, Guangzhou, China). All mice were housed in specific-pathogen-free facilities and in accordance with the National Animal Care and Use Committee. All animal experiments were approved by the Institutional Laboratory Animal Care and Use Committee of Soochow University (Suzhou, China).

Two murine HCC models were established in the study. To generate the orthotopic HCC model by hydrodynamic injection, 1×10^6 hepa1-6 cells in 2 ml PBS were injected via tail vein within 8 to 10 s. Mice were sacrificed 3 weeks later, and tumor nodules were counted. The DEN-induced spontaneous HCC model was generated by injecting 14-day-old C57BL/6 mice with 25 mg/kg DEN (Sigma-Aldrich, St Louis, MO). Eight months later, mice were sacrificed, and the livers were removed. Tumor size was measured, and the number of tumor nodules was counted.

Flow cytometry

For cell-surface staining, cells were blocked with CD16/32 FcR-block (BioLegend, San Diego, CA) for 15 min, and stained with fluorescent dye-conjugated mAb for 30 min at 4°C. For intracellular cytokine staining, cells were stimulated for 4–6 h with PMA (50 ng/ml) and ionomycin (500 ng/ml) in the presence of brefeldin A (10 μg/ml; BD Bio- sciences, San Jose, CA). Cells were stained for surface markers for 30 min, then fixed with 4% paraformaldehyde, permeabilized with 1% saponin (Sigma-Aldrich, St Louis, MO), and stained for cytokines for 30 min at 4°C. The antibodies used for FACS staining were FITC-anti-mouse-NK1.1 (PK136), PE/CF594-anti-mouse-CD3 (145-2C11), PE/CF594-anti-mouse-CD45 (30-F11), PerCP/Cy5.5-anti-mouse-CD4 (RM4–5), PerCP/Cy5.5-anti- mouse-NK1.1 (PK136), PE/CY7-anti-mouse-CD19 (1D3), APC/H7-anti-mouse-CD4 (GK1.5), and ACP/Cy7-anti-mouse-CD11b (M1/70) were purchased from BD Bioscience (San Jose, CA). The FITC-anti-mouse-CD8 (53–6.7), FITC-anti-mouse-I-A/I-E (M5/114.15.2), FITC- anti-mouse-CD4 (GK1.5), PE-anti-mouse-Ly6G (1A8), PE-anti- mouse-CD4 (RM4-5), PE-anti-mouse-NK1.1 (PK136), PE-anti-mouse-IFN-γ (XMG1.2), PE-Rat-IgG2b, kappa Isotype (RTK4530), PE/Dazzle594-anti-mouse-CD45 (30-F11), PerCP/Cy5.5-anti-mouse-TCRγδ (GL3), PerCP/Cy5.5- anti-mouse-IL-17A (TC11-18H10.1), PerCP/Cy5.5-anti-mouse-CD45.1 (A20), APC-anti-mouse-CD8 (53–6.7), APC-anti-mouse-CD4 (RM4-5), APC-anti-mouse-F4/80 (BM8), Alexa fluor 700-anti-mouse-CD45 (30-F11), APC-anti-mouse- IFN-γ (XMG1.2), PE/Cy7-anti-mouse-TNF-α (MP6-XT22), and PE/Cy7- anti-mouse-Ly6C(HK1.4), PE/Cy7-anti-mouse-CD44 (IM7), APC/Cy7-anti-mouse-CD11b (M1/70), APC/Cy7-anti-mouse-CD62L (MEL-14), Brilliant Violet421-anti-mouse CD8a (53 – 6.7), Brilliant Violet510-anti-mouse CD3ε (145-2C11), Brilliant Violet510-anti-mouse CD11c (N418) were purchased from BioLegend (San Diego, CA).

Neutralization of IL-27 in vivo.

To neutralize IL-27 *in vivo*, mice were injected i.p. with anti-IL-27p28 50ug (R&D Systems, Minneapolis, MN) per mouse immediately after the tumor cell inoculation on day 0 and one week later. Monoclonal goat IgG (Bio X Cell, Lebanon, NH) were used as isotype control.

Fecal transplantation

Fecal pellets from WT and Itgax-IL-27p28$^{f/f}$ mice were collected, and each fecal pellet was resuspended in 1ml PBS. The suspension from each fecal pellet was used for oral gavage of one recipient mouse at 200ul per gavage. Mice were gavaged with WT or Itgax-IL-27p28$^{f/f}$ mice fecal suspension or PBS as control every other day for one week prior to tumor inoculation and once a week on day 7 and day 14 post tumor implantation.

Bacterial gavage

Bifidobacterium species including *B. bifidum, B. longum, B. lactis* and *B. breve* were purchased from China General MicroBiological Culture Collection Center (BeiJing, China). Bacteria were cultured in an anaerobic chamber according to manufacturer's instructions. To confirm the compositions, bacteria were harvested and washed with PBS and centrifuged at 3000 rpm for 30 minutes. The pellet was sent for sequencing (GENEWIZ, Suzhou, China). For bacteria transplantation, a cocktail of Bifidobacterium

species was resuspended in PBS at $5x10^9$ CFU/ml. Each mouse was given 200µl of Bifidobacterium ($1x10^9$ CFU/mouse) by oral gavage with the same schedule as fecal transplant.

Fecal sample processing, sequencing, and analysis

Mice feces were collected into autoclaved EP tube and stored at − 80°C. Extracted DNA samples were amplified, DNA libraries were constructed, and the sequencing 16S rRNA was performed on Illumina MiSeq platform (GENEWIZ, Beijing, China). Sequences were grouped into operational taxonomic units (OTUs) using the clustering program VSEARCH (1.9.6) against the Silva 132 database pre-clustered at 97% sequence identity. The Ribosomal Database Program (RDP) classifier was used to assign taxonomic category to all OTUs at confidence threshold of 0.8. The RDP classifier uses the Silva 132 database which has taxonomic categories predicted to the species level. Base on the OUT analysis results obtained, Shannon index and Chao1 index, coordinates analysis (PCoA) were conducted by R package to display microbiome space between samples. A heatmap of the identified key variables was completed by the Heat map builder.

Bifidobacterium bacteria were harvested and centrifuged to collect the pellet. Bacterial 16S rRNA were amplified and sequenced (GENEWIZ, Beijing, China). Briefly, 16S rRNA was amplified from extracted DNA using broad-range bacterial primers 27F and 1492R. Amplified products from samples were verified by gel electrophoresis using the PCR reaction mixture in agarose gels. The 16Sr RNA was sequenced by Sanger Sequencing. The sequencing data was blasted in NCBI database for confirmation.

Activation of T cells with OVA peptide-pulsed TIP-DCs

TIP-DCs (CD45 + CD11b + Ly6C+) were sorted using a FACSAria III flow cytometer (BD Biosciences, San Jose, CA) and pulsed with 10 µg/ml OVA peptide for 2 hr at 37° in a total volume of 1 ml, then washed four times in RPMI-1640. In addition, $CD8^+$ T cells from OT-I mice were separated by using mouse CD8 isolation cocktail kits, respectively (Stem cell, Vancouver, BC). $CD8^+$ T cells in the suspension were then isolated and co-cultured with TIP-DC pulsed with or without OVA peptides (10 ug/ml, Sigma-Aldrich, St. Louis, MO) in a 96-well at a ratio of 3:1. After three days, production of IFN-γ and TNF-α by CD8 + T cells was analyzed by flow cytometry.

T cell proliferation assays

$CD8^+$ T cells from OT-I mice were separated by using mouse $CD8^+$ isolation cocktail kits, respectively (Stem cell, Vancouver, BC). Sorted $CD8^+$ T cells were labeled with CFSE (ThermoFisher, Grand Island, NY) according to the manufacturer's instructions. Briefly, cells were resuspended in 50ml PBS and centrifuged for 5 minutes at 300g. Cells were then resuspended in 10 ml of 5 µM CellTrace CFSE staining solution and incubated in a 37°C water bath for 20 minutes. Then 40 ml serum-free RPMI-1640 medium was added, and cells were incubated for 5 minutes. After incubation, cells were centrifuged for 5 minutes at 300g and resuspended in serum-free RPMI-1640 medium. CFSE-labeled $CD8^+$ T cells were seeded in anti-CD3 (5ug/ml, Biolegend, San Diego, CA) and anti-CD28 (2ug/ml, Biolegend, San Diego, CA) pre-coated 96-well plate and cultured in the presence of various concentrations of IL-27. After three day, CFSE

expression on $CD8^+$ T cells was analyzed by flow cytometry. In some experiments, CFSE-labeled $CD8^+$ T cells were co-cultured with TIP-DCs pulsed with OVA peptides in 96-well plates at a ratio of 3:1. After three days, CFSE expression on $CD8^+$ T cells was analyzed by flow cytometry.

Statistical analysis

Multiple comparisons were performed using one-way ANOVA with Tukey's post-hoc test when comparing among all groups or Dunnett's post-hoc test when comparing to control only. Comparisons between two groups were performed using Students' unpaired t-test. All statistical analyses were performed with Graphpad Prism version 7 (GraphPad Software, San Diego, CA). Data were shown as mean ± SEM, and $p < 0.05$ was considered statistically significant. * indicates $p < 0.05$, ** indicates $p < 0.01$, *** indicates $p < 0.001$.

Results

DC-derived IL-27 promoted tumor development in murine HCC models

To investigate the role of DC-derived IL-27 in tumor development, orthotopic murine HCC model was established as previously described by hydrodynamic injection (HGT) of hepa1-6 cells into wild-type (WT) or IL-27p28 DC conditional knockout (Itgax-IL-$27p28^{f/f}$) mice. Tumor growth was significantly reduced in the liver of Itgax-IL-$27p28^{f/f}$ mice compared with the WT mice (Fig. 1a-b). To further confirm the result, we chemically induced HCC with diethyl nitrosamine (DEN) in both WT and Itgax-IL-$27p28^{f/f}$ mice (Fig. 1c-d). Smaller and fewer tumor nodules were observed in Itgax-IL-$27p28^{f/f}$ mice than in WT mice, indicating that DC-derived IL-27p28 promoted tumor development in murine HCC models. Furthermore, we neutralized IL-27 by using anti-IL-27p28 (Anti-p28) antibody in orthotopic HCC model (Fig. 1e-f). As expected, mice treated with anti-p28 antibodies developed fewer tumor nodules compared with the isotype control-treated mice. Taken together, these results demonstrated that DC-derived IL-27 promoted tumor growth in murine HCC models.

DC-derived IL-27 inhibited T cell activation in the tumor microenvironment

To elucidate the anti-tumor immune response regulated by DC-derived IL-27, we examined the percentages and numbers of T cells and NK cells in the spleen and liver of WT and Itgax-IL-$27p28^{f/f}$ tumor bearing mice in orthotopic HCC model (Fig. 2a-d). While there was no significant difference in the spleen, both frequencies and numbers of T cells were significantly increased in the liver of Itgax-IL-$27p28^{f/f}$ mice compared with WT mice. Among the T cells, both $CD4^+$ T and $CD8^+$ T cells were increased. The effector $CD4^+$ T cells also exhibited higher percentages in the spleen, and both higher percentages and numbers in the liver of Itgax-IL-$27p28^{f/f}$ mice (Fig. 2e-h). The percent and number of effector $CD8^+$ T

cells were increased in both spleen and liver of Itgax-IL-27p28$^{f/f}$ mice compared with the WT (Fig. 2e-h), suggesting that DC-derived IL-27 may suppress T cell function, especially at the tumor site.

To further assess the anti-tumor function of the immune effector cells, we examined the cytokine production by CD4$^+$ T, CD8$^+$ T and NK cells using flow cytometry (Fig. 2i-l). The percentages of IFN-γ- and TNF-α-producing CD8$^+$ T cells were significantly increased in the spleen of Itgax-IL-27p28$^{f/f}$ mice compared with the WT mice. Moreover, the percentages and numbers of IFN-γ- and TNF-α-producing CD4$^+$ T cells and CD8$^+$ T cells were greatly increased in the liver of Itgax-IL-27p28$^{f/f}$ mice compared with the WT mice. The percent and number of TNF-α-producing NK cells were also increased in the liver of Itgax-IL-27p28$^{f/f}$ mice. We further confirmed the tumor-promoting role of DC-derived IL-27 in a melanoma lung metastasis model (Fig. S1a). There was an increase in CD8$^+$T cell percentages and both effector CD4$^+$T and CD8$^+$T cell percentages were increased in the lung (Fig. S1b-c). Thus, in the absence of DC-derived IL-27, both CD4$^+$ T and CD8$^+$ T cells had enhanced immune activation phenotypes and increased IFN-γ and TNF-α production especially in the tumor microenvironment.

DC-derived IL-27 promoted the expression of inhibitory receptors on both CD4 $^+$ and CD8$^+$ T cells in tumor-bearing mice

Immune checkpoint inhibitors are usually highly expressed on T cells in the tumor microenvironment. It has been shown that IL-27 signaling is essential for inducing T-cell immunoglobulin and mucin-domain containing-3 (Tim3)$^+$ exhausted T cells[21]. The expression of co-inhibitory receptors on CD4$^+$ and CD8$^+$ T cells is also found to be driven by IL-27 by a study using single-cell mass cytometry[28]. We then examined the expression of programmed cell death protein 1 (PD-1) and Tim-3 on CD4$^+$ T cells and CD8$^+$ T cells in naïve and tumor-bearing WT and Itgax-IL-27p28$^{f/f}$ mice. There was no PD-1 or Tim-3 expression on CD4$^+$ and CD8$^+$ T cells in spleen and liver of naïve WT and Itgax-IL-27p28$^{f/f}$ mice (Fig. 3a). As expected, PD-1 and Tim3 were expressed at a relatively higher level on both CD4$^+$ and CD8$^+$ T cells in tumor-bearing liver than in spleen of WT mice (Fig. 3b-g). Interestingly, this increased PD-1 and Tim3 expression on T cells in the tumor microenvironment was completely abolished in the absence of DC-derived IL-27 in the Itgax-IL-27p28$^{f/f}$ mice (Fig. 3b-g). This was also observed in the melanoma lung metastasis model (Fig. S1d). These results demonstrated that DC-derived IL-27 is essential in the upregulation of inhibitory receptor expression on T cells in the tumor microenvironment.

DC-derived IL-27 promoted tumor development through modulating gut microbiota

Many studies have demonstrated the important roles of gut microbiota in viral infections, autoimmune diseases, and tumor development[49–51]. In addition, there could be bidirectional crosstalk occurring between the liver and gut[52]. To address whether gut microbiota could play a role in IL-27-mediated immune suppression and tumor development, we collected feces from WT and Itgax-IL-27p28$^{f/f}$ mice and

transplanted into Itgax-IL-27p28$^{f/f}$ and WT mice respectively by gavage with PBS as control (Fig. 4a-b). Interestingly, tumor growth in WT mice was significantly inhibited after receiving Itgax-IL-27p28$^{f/f}$ feces, while the tumor growth in Itgax-IL-27p28$^{f/f}$ mice was not affected by WT fecal transfer. These results suggest that the tumor-suppressive immune mechanism in Itgax-IL-27p28$^{f/f}$ mice can be mediated and transferred through gut microbiota.

To identify specific bacteria stains involved in promoting anti-tumor immune responses, we examined the fecal bacterial content of WT and Itgax-IL-27p28$^{f/f}$ mice with or without fecal transplant using 16s ribosomal RNA (rRNA) miSeq Illumina platform (Fig. 4c-h). The shared bacteria genera were shown in the Veen diagram, which indeed demonstrated a distinct difference in gut bacteria compositions between WT and Itgax-IL-27p28$^{f/f}$ mice (Fig. 4c). Principal coordinate analysis revealed that samples from WT mice receiving Itgax-IL-27p28$^{f/f}$ fecal material became more like samples obtained from Itgax-IL-27p28$^{f/f}$ mice, suggesting the gut microbiota modulation via gavage was successfully performed (Fig. 4d). In contrast, Itgax-IL-27p28$^{f/f}$ mice receiving WT fecal material did not significantly change in gut bacterial composition, which is consistent with the results of tumor growth, suggesting the gut bacteria in Itgax-IL-27p28$^{f/f}$ mice may be dominant over those in WT mice. The result analyzed by unweighted pair group method with arithmetic mean (UPGMA) further confirmed the finding that WT mice receiving Itgax-IL-27p28$^{f/f}$ fecal material became similar to Itgax-IL-27p28$^{f/f}$ mice in their gut bacterial composition, whereas WT mice feces transplant did not significantly modify the gut microbiota of the Itgax-IL-27p28$^{f/f}$ mice (Fig. 4e). The indices for community diversity and richness were calculated and described as Shannon index and Chao1 index respectively (Fig. 4f). The diversity and richness of gut bacterial community were decreased in Itgax-IL-27p28$^{f/f}$ mice. Receiving fecal material from Itgax-IL-27p28$^{f/f}$ mice decreased the community richness and diversity in WT mice, while receiving fecal material from WT mice increased the community richness and diversity in Itgax-IL-27p28$^{f/f}$ mice, especially as shown in Chao1 index. Taken together, these results demonstrated that the gut bacterial compositions are significantly different between WT and Itgax-IL-27p28$^{f/f}$ mice, and the tumor-promoting immune mechanism in the absence of DC-derived IL-27 could be mediated by gut microbiota.

Since the diversity and richness of the bacterial community could be modified in the Itgax-IL-27p28$^{f/f}$ mice receiving WT fecal materials, but the tumor growth was not affected, the tumor growth phenotypes are more likely to be related to the bacterial composition than the diversity and richness. To further identify the difference in bacterial composition, we analyzed for differentially abundant taxa across all permutations between various groups of mice (Fig. 4g). Taxonomically, nine different bacterial phyla including *Actinobacteria, Bacteroidetes, Cyanobacteria, Deferribacteres, Firmicutes, Proteobacteria, Saccharibacteria, Tenericutes, and Verrucomicrobia* were identified. We further narrowed down to genus-level taxa that have been associated with anti-tumor effects. Bifidobacterium, Parasutterella and Akkermansia, which belong to *Actinobacteria*, *Proteobacteria* and *Verrucomicrobia* respectively and have been associated with anti-tumor functions, were increased in all groups of Itgax-IL-27p28$^{f/f}$ mice, Itgax-IL-27p28$^{f/f}$ mice receiving WT feces, and WT mice receiving Itgax-IL-27p28$^{f/f}$ feces compared to WT mice

(Fig. 4h-i). Among them, Bifidobacterial has been well studied for its role in activating host immune responses[40]. To establish its role in our murine HCC model, we inoculated a cocktail of Bifidobacterium species, including B.bifidum, B.longum, B.breve and B.lactis to tumor-bearing mice by gavage (Fig. 4j). Treatment with Bifidobacterium significantly inhibited tumor growth compared with the control group. To exclude any possible influence of tumor growth on gut microbiota, we also examined the fecal bacterial content of naïve WT and Itgax-IL-27p28$^{f/f}$ mice which exhibited similar differences, suggesting the changes in microbiota were induced by intrinsic expression of DC-derived IL-27 (Fig. S2). Taken together, these results demonstrated that DC-derived IL-27 could promote tumor growth and suppress anti-tumor immune responses through the modulation of gut microbiota.

Ly6C $^+$ MHCII $^+$ (TIP)-DCs could be modulated by gut microbiota in the absence of DC-derived IL-27 to promote T cell functions

Gut microbiota has been shown to modulate DC phenotypes and functions. Depletion of gut microbiota using antibiotic cocktail could reduce Ly6C$^+$MHC II$^+$ cells[53]. Bifidobacterium could increase the MHC II$^+$ DCs in the tumor microenvironment to promote anti-tumor immune response[40]. Thus, we hypothesis that DC-derived IL-27 may regulate DC function via modulation of gut microbiota. To address this, we first examined the major myeloid cell subsets in spleen and liver of WT and Itgax-IL-27p28$^{f/f}$ mice including DCs, myeloid-derived suppressor cells (MDSCs), and macrophages (Fig. 5a-d). There was a slight decrease of DCs in the spleen of Itgax-IL-27p28$^{f/f}$ mice compared to WT mice, while no difference was observed in tumor-bearing liver. The expressions of CD80, CD86 or MHC II were similar between WT and Itgax-IL-27p28$^{f/f}$ mice on DCs, MDSCs, and macrophages both in spleen and liver (Fig. 5b, 5d-f). However, both percentages of CD11b$^+$Ly6G$^-$Ly6C$^+$MHC II$^+$ DC population out of CD11b$^+$Ly6G$^-$Ly6C$^+$ population or total leukocyte were significantly increased in the liver of Itgax-IL-27p28$^{f/f}$ mice compared with WT mice (Fig. 5g). This DC population has been previously reported as tumor necrosis factor and inducible nitric-oxide-synthase-producing DCs (TIP-DC)[34]. TIP-DCs have high level expression of MHCII and CD86 and play a role in immune responses against bacterial infection and tumor by enhancing T cell priming [54,55]. To confirm that TIP-DC could be modulated by gut microbiota, we examined this population in WT and Itgax-IL-27p28$^{f/f}$ mice receiving fecal transplant (Fig. 5h). The level of MHC class II expression on the CD11b$^+$Ly6G$^-$Ly6C$^+$ population from tumor-bearing liver was higher in Itgax-IL-27p28$^{f/f}$ mice than in WT mice, and its expression was significantly increased in WT mice receiving Itgax-IL-27p28$^{f/f}$ fecal materials compared to PBS control, suggesting that MHC class II expression on TIP-DCs could be modulated by gut microbiota.

We then investigated whether TIP-DCs from WT or Itgax-IL-27p28$^{f/f}$ mice were different in their functions of priming T cells. To exclude the direct effect of IL-27 on T cells, we treated native CD8$^+$ T cells activated with anti-CD3/anti-CD28 with or without recombinant IL-27 (Fig. 6a). No difference was observed in T cell proliferation in the presence or absence of IL-27. We then isolated TIP-DCs from WT or Itgax-IL-27p28$^{f/f}$ tumor-bearing mice by flow sorting and pulsed them with OVA antigen (Fig. 6b). CD8$^+$ T cells from OT-1

mice were co-cultured with OVA-pulsed TIP-DCs for three days and analyzed for proliferation and TNF-α and IFN-γ production. The proliferation of the $CD8^+$ T cells measured by CFSE labelling was enhanced by TIP-DCs from Itgax-IL-$27p28^{f/f}$ mice compared with the WT control (Fig. 6c). $CD8^+$ T cells stimulated by TIP-DCs from Itgax-IL-$27p28^{f/f}$ mice produced significantly higher level of TNF-α and IFN-γ compared with the WT control (Fig. 6d). These results demonstrated that in the absence of DC-derived IL-27, TIP-DCs' function of priming T cells was significantly promoted. Taken together, these results suggest that TIP-DCs could be modulated by gut microbiota in the absence of DC-derived IL-27 to promote anti-tumor T cell functions.

Discussion

The role of IL-27 in tumor development has been controversial. In the current study, we investigated the function of DC-derive IL-27 in murine HCC models and found that it promoted HCC tumor development and suppressed anti-tumor immune response. Interestingly, the tumor growth phenotype of Itgax-IL-$27p28^{f/f}$ mice could be transferred via gut microbiota, and some bacteria strains were identified in the gut of Itgax-IL-$27p28^{f/f}$ mice that could inhibit tumor development and were significantly reduced in the WT mice. Furthermore, the percentage and MHC class II expression of TIP-DCs were increased, and their T cell-activating function was enhanced in Itgax-IL-$27p28^{f/f}$ mice compared with the WT mice. The phenotypes of the TIP-DCs could be modulated by gut microbiota. Therefore, our results have uncovered a novel mechanism of DC-derived IL-27 regulating anti-tumor immune response via modulation of gut microbiota and provided new insights to the function of DC-derived cytokines in adaptive immune responses.

Both tumor-suppressive and tumor-promoting functions of IL-27 have been described in the previous studies. IL-27 has been shown to activate STAT1 signaling and promote IFN-γ production[16]. Many studies demonstrated that IL-27 could inhibit tumor growth and promote anti-tumor immunity by upregulating Th1 and CTL responses in tumor models such as neuroblastoma, colon carcinoma, and B16 melanoma[24,25,27]. On the other hand, IL-27 has been shown to act as a negative regulator of T cell responses in IL-$27ra^{f/f}$ mice challenged with viral, bacterial or parasitic pathogens[16,56,57]. Moreover, IL-27 could promote tumor progression by inducing an immune-suppressive phenotype in tumor-associated macrophage and promoting co-inhibitory receptor Tim-3 expression on T cells[21,23]. Recently, the single-cell mass cytometry results also revealed that co-inhibitory receptor expression on T cells is driven by IL-27[28]. Currently, SRF388, an IL-27 neutralizing antibody, is currently being evaluated in a Phase I study in patients with advanced solid tumors, including HCC (#NCT04374877). In fact, IL-27 is expressed at a relatively higher level in liver than in other organs (http://gepia2.cancer-pku.cn/#general). Its expression has also been shown to be increased in patients infected with hepatitis B virus[58–60], which is one of the important inducing factors in liver carcinogenesis[61]. The levels of IL-27 in pre-diagnostic sera were significantly associated with increased risk of HCC development[62], suggesting IL-27 could play an important role in liver chronic inflammation and carcinogenesis. We found that DC-derived IL-27 could

promote tumor development and suppress anti-tumor adaptive immune response. A previous study using the same IL-27p28 conditional knockout mice showed tumor-suppressive role of DC-derived IL-27 in a subcutaneous melanoma model[27]. However, DC-derived IL-27 promoted melanoma lung metastasis and suppressed anti-tumor immune response in the lung (Fig. S1), suggesting the role of IL-27 regulating anti-tumor immune response could be organ-specific. The direct or indirect effects of IL-27 on the immune responses may be proportionally different depending on the tissue-specific environment.

In murine HCC models, the activation and cytokine production by both $CD4^+$ and $CD8^+$ T cells were enhanced in the absence of DC-derived IL-27. Many previous studies have demonstrated an important role of IL-27 in T cell activation and differentiation promoting Th1 phenotype and CTL self-renewal[16,63–65]. The immune-suppressive function of IL-27 we observed in HCC models could be due to the indirect effect of IL-27 on T cells that is dominant in the liver tumor microenvironment. It has been shown that IL-27 could induce co-inhibitory receptor expression on T cells, such as PD-1 and Tim-3, in many tumor models[21,28,66]. We also demonstrated that $CD4^+$ and $CD8^+$ T cells expressed high level of PD-1 in tumor-bearing livers in WT mice while the expression was greatly diminished in Itgax-IL-27p28$^{f/f}$ mice. However, the mechanism of IL-27 inducing inhibitory receptor expression on T cells needs further investigation.

The link between gut microbiota and tumor development has been demonstrated in many tumor types, including melanoma, prostate cancer and lymphoma[35,40,42,67]. Due to the close anatomical and functional relationship between liver and gut, gut microbiota has been shown to play a role in HCC development[45,46]. Interestingly, we found the tumor-suppressive phenotype of Itgax-IL-27p28$^{f/f}$ mice could be transferred to WT mice by fecal transplantation. However, Itgax-IL-27p28$^{f/f}$ mice receiving WT fecal materials did not exhibit significant changes in their gut microbiota composition and tumor development, suggesting the bacterial strains that were present in the gut of Itgax-IL-27p28$^{f/f}$ mice might be dominant when coexisting with those from the WT mice. The diversity and richness were decreased in Itgax-IL-27p28$^{f/f}$ mice compared with the WT mice. Tumor growth could be inhibited with lower microbiota diversity and richness in mice that are treated with antibiotic cocktail (ABX)[41]. Many studies also suggest that microbiota diversity could be used to predict cancer progression[68–70]. However, we found Itgax-IL-27p28$^{f/f}$ mice that received WT fecal materials increased the diversity and richness compared to PBS-treated Itgax-IL-27p28$^{f/f}$ mice but had similar tumor growth. Thus, diversity and richness may not be the only indicator and the composition of the gut microbiota could be more critical in modulating tumor development. Bifidobacterium and Akkermansia were increased in the gut of Itgax-IL-27p28$^{f/f}$ mice compared with WT mice. Both are found to play important roles in tumor development and treatment response[40,44,71,72,65]. However, our results do not rule out the possible contributions of other commensal bacteria species affected by IL-27, and how IL-27 regulates gut microbiota needs further investigation.

We discovered that the population of $CD11b^{+}Ly6G^{-}Ly6C^{+}MHC\ II^{+}$ cells were significantly increased in Itgax-IL-$27p28^{f/f}$ mice. Moreover, the MHC II expression on these cells could be modulated by fecal transplantation which is consisted with previous finding showing that the gut microbiota could affect MHC II expression on $CD11b^{+}Ly6C^{+}$ cells[40]. This population has been given a name of TIP-DC[54,35]. TIP-DCs have been shown to play an important role in protecting the host from bacteria infection[35,73], viral infection[74] and tumor growth[75]. In TIP-DC mediated anti-tumor responses, they are essential in $CD8^{+}$T cells activation[75] and enhanced cytotoxicity[54]. By co-culture experiments, we also demonstrated that TIP-DCs from Itgax-IL-$27p28^{f/f}$ mice are more competent in promoting $CD8^{+}$ T cell proliferation and cytokine production, suggesting that they could be the link between modified gut microbiota and enhanced adaptive anti-tumor immune response.

Conclusions

Our results demonstrated that DC-derived IL-27 could promote tumor growth and suppress anti-tumor immune response in murine HCC through the modulation of gut microbiota. This indirect effect of IL-27 on adaptive immune response provides insights into possible organ-specific functions of IL-27 and targeting IL-27 in tumor immunotherapy.

Abbreviations

HCC: Hepatocellular carcinoma

DC: Dendritic cell

Itgax-IL-$27p28^{f/f}$: IL-27p28 DC-conditional knockout

TIP-DC: Tumor necrosis factor and inducible nitric-oxide-synthase-producing DC.

CNTF: Ciliary neurotrophic factor

CT1: Cardiotrophin1

CLCF1: Cardiotrophin-like cytokine factor 1

LIF: Leukemia inhibitory factor

EAE: Experimental autoimmune encephalomyelitis

IBD: Inflammatory bowel disease

OT-I mice: C57BL/6-Tg(TcraTcrb)1100Mjb/J mice

OTUs: Operational taxonomic units

WT: Wild-type

HGT: Hydrodynamic injection

Anti-p28: Anti-IL-27p28

Tim3: T-cell immunoglobulin and mucin-domain containing-3

PD-1: Programmed cell death protein 1

rRNA: Ribosomal RNA

UPGMA: Unweighted pair group method with arithmetic mean

ABX: Antibiotic cocktail

Declarations

Ethics approval and consent to participate:

Not applicable.

Consent for publication:

Not applicable.

Availability of data and materials:

RNA-Seq data that support the findings of this study are available from the corresponding author upon request. The authors declare that the data supporting the findings of this study are available within the article and provided as Source Data file.

Competing interests:

The authors declare that they have no competing interests.

Funding:

This work has been supported by China Postdoctoral Science Foundation (2019M661938), Jiangsu Planned Projects for Postdoctoral Research Funds (2019K098), Natural Science Foundation of Jiangsu Higher Education Institutes (20KJD320001), Translational Research Grant of NCRCH (2021ZKQC01), Life Science Institute Grand Challenge Fund, and the start-up grant of National University of Singapore.

Author contributions:

Y.L, Y.S, and H.L designed the research. Y.L, Y.S, Z.J and H.G performed the experiments and analyzed the data. L.L, Y.Z, Y.M and HY.T assisted in the experiments. Z.Y provided Itgax-IL-27p28$^{f/f}$ mice and OT-I mice. D.W and H.L supervised the study. Y.L, Y.S, and H.L wrote the manuscript.

Acknowledgements:

Not applicable.

Authors' information:

Not applicable.

References

1. Khatib, S., Pomyen, Y., Dang, H. & Wang, X. W. Understanding the Cause and Consequence of Tumor Heterogeneity. Trends Cancer 2020; 6l, 267–271.
2. Wu, S., Zhu, W., Thompson, P. & Hannun, Y. A. Evaluating intrinsic and non-intrinsic cancer risk factors. *Nat Commun* 2018; 9l, 3490.
3. Hanahan, D. & Weinberg, R. A. Hallmarks of cancer: the next generation. Cell 2011; 144l, 646–674.
4. Jones, S. A. & Jenkins, B. J. Recent insights into targeting the IL-6 cytokine family in inflammatory diseases and cancer. Nat Rev Immunol 2018; 18l, 773–789.
5. Kumari, N., Dwarakanath, B. S., Das, A. & Bhatt, A. N. Role of interleukin-6 in cancer progression and therapeutic resistance. Tumour Biol 2016; 37l, 11553–11572.
6. Rokavec, M., Oner, M. G., Li, H., Jackstadt, R., Jiang, L., Lodygin, D. *et al.* IL-6R/STAT3/miR-34a feedback loop promotes EMT-mediated colorectal cancer invasion and metastasis. J Clin Invest 2014; 124l, 1853–1867.
7. Yadav, A., Kumar, B., Datta, J., Teknos, T. N. & Kumar, P. IL-6 promotes head and neck tumor metastasis by inducing epithelial-mesenchymal transition via the JAK-STAT3-SNAIL signaling pathway. Mol Cancer Res 2011; 9l, 1658–1667.
8. Ernst, M. & Putoczki, T. L. Targeting IL-11 signaling in colon cancer. Oncotarget 2013; 4l, 1860–1861.
9. Tye, H., Kennedy, C. L., Najdovska, M., McLeod, L., McCormack, W., Hughes, N. *et al.* STAT3-driven upregulation of TLR2 promotes gastric tumorigenesis independent of tumor inflammation. Cancer Cell 2012; 22l, 466–478.
10. Tugues, S., Burkhard, S. H., Ohs, I., Vrohlings, M., Nussbaum, K., Vom Berg, J. *et al.* New insights into IL-12-mediated tumor suppression. Cell Death Differ 2015; 22l, 237–246.
11. Pflanz, S., Timans, J. C., Cheung, J., Rosales, R., Kanzler, H., Gilbert, J. *et al.* IL-27, a heterodimeric cytokine composed of EBI3 and p28 protein, induces proliferation of naive CD4 + T cells. *Immunity* 2002; 16l, 779–790.
12. West, N. R. Coordination of Immune-Stroma Crosstalk by IL-6 Family Cytokines. *Front Immunol* 2019; 10l, 1093.

13. Hibbert, L., Pflanz, S., De Waal Malefyt, R. & Kastelein, R. A. IL-27 and IFN-alpha signal via Stat1 and Stat3 and induce T-Bet and IL-12Rbeta2 in naive T cells. J Interferon Cytokine Res 2003; 23l, 513–522.
14. Lucas, S., Ghilardi, N., Li, J. & de Sauvage, F. J. IL-27 regulates IL-12 responsiveness of naive CD4 + T cells through Stat1-dependent and -independent mechanisms. Proc Natl Acad Sci U S A 2003; 100l, 15047–15052.
15. Takeda, A., Hamano, S., Yamanaka, A., Hanada, T., Ishibashi, T., Mak, T. W. *et al.* Cutting edge: role of IL-27/WSX-1 signaling for induction of T-bet through activation of STAT1 during initial Th1 commitment. J Immunol 2003; 170l, 4886–4890.
16. Hamano, S., Himeno, K., Miyazaki, Y., Ishii, K., Yamanaka, A., Takeda, A. *et al.* WSX-1 is required for resistance to Trypanosoma cruzi infection by regulation of proinflammatory cytokine production. Immunity 2003; 19l, 657–667.
17. Villarino, A., Hibbert, L., Lieberman, L., Wilson, E., Mak, T., Yoshida, H. *et al.* The IL-27R (WSX-1) is required to suppress T cell hyperactivity during infection. Immunity 2003; 19l, 645–655.
18. Hall, A. O., Beiting, D. P., Tato, C., John, B., Oldenhove, G., Lombana, C. G. *et al.* The cytokines interleukin 27 and interferon-gamma promote distinct Treg cell populations required to limit infection-induced pathology. Immunity 2012; 37l, 511–523.
19. Batten, M., Li, J., Yi, S., Kljavin, N. M., Danilenko, D. M., Lucas, S. *et al.* Interleukin 27 limits autoimmune encephalomyelitis by suppressing the development of interleukin 17-producing T cells. Nat Immunol 2006; 7l, 929–936.
20. Villarino, A. V., Artis, D., Bezbradica, J. S., Miller, O., Saris, C. J., Joyce, S. *et al.* IL-27R deficiency delays the onset of colitis and protects from helminth-induced pathology in a model of chronic IBD. Int Immunol 2008; 20l, 739–752.
21. Zhu, C., Sakuishi, K., Xiao, S., Sun, Z., Zaghouani, S., Gu, G. *et al.* An IL-27/NFIL3 signalling axis drives Tim-3 and IL-10 expression and T-cell dysfunction. *Nat Commun* 2015; 6l, 6072.
22. Ma, Q. Y., Huang, D. Y., Zhang, H. J., Wang, S. & Chen, X. F. Function and regulation of LAG3 on CD4(+)CD25(-) T cells in non-small cell lung cancer. Exp Cell Res 2017; 360l, 358–364.
23. Park, Y. J., Ryu, H., Choi, G., Kim, B. S., Hwang, E. S., Kim, H. S. *et al.* IL-27 confers a protumorigenic activity of regulatory T cells via CD39. Proc Natl Acad Sci U S A 2019; 116l, 3106–3111.
24. Salcedo, R., Stauffer, J. K., Lincoln, E., Back, T. C., Hixon, J. A., Hahn, C. *et al.* IL-27 mediates complete regression of orthotopic primary and metastatic murine neuroblastoma tumors: role for CD8 + T cells. J Immunol 2004; 173l, 7170–7182.
25. Hisada, M., Kamiya, S., Fujita, K., Belladonna, M. L., Aoki, T., Koyanagi, Y. *et al.* Potent antitumor activity of interleukin-27. Cancer Res 2004; 64l, 1152–1156.
26. Matsui, M., Kishida, T., Nakano, H., Yoshimoto, K., Shin-Ya, M., Shimada, T. *et al.* Interleukin-27 activates natural killer cells and suppresses NK-resistant head and neck squamous cell carcinoma through inducing antibody-dependent cellular cytotoxicity. Cancer Res 2009; 69l, 2523–2530.

27. Wei, J., Xia, S., Sun, H., Zhang, S., Wang, J., Zhao, H. *et al.* Critical role of dendritic cell-derived IL-27 in antitumor immunity through regulating the recruitment and activation of NK and NKT cells. J Immunol 2013; 191l, 500–508.
28. Chihara, N., Madi, A., Kondo, T., Zhang, H., Acharya, N., Singer, M. *et al.* Induction and transcriptional regulation of the co-inhibitory gene module in T cells. Nature 2018; 558l, 454–459.
29. Mazmanian, S. K., Liu, C. H., Tzianabos, A. O. & Kasper, D. L. An immunomodulatory molecule of symbiotic bacteria directs maturation of the host immune system. Cell 2005; 122l, 107–118.
30. Olin, A., Henckel, E., Chen, Y., Lakshmikanth, T., Pou, C., Mikes, J. *et al.* Stereotypic Immune System Development in Newborn Children. Cell 2018; 174l, 1277–1292 e1214.
31. Deshmukh, H. S., Liu, Y., Menkiti, O. R., Mei, J., Dai, N., O'Leary, C. E. *et al.* The microbiota regulates neutrophil homeostasis and host resistance to Escherichia coli K1 sepsis in neonatal mice. Nat Med 2014; 20l, 524–530.
32. Geva-Zatorsky, N., Sefik, E., Kua, L., Pasman, L., Tan, T. G., Ortiz-Lopez, A. *et al.* Mining the Human Gut Microbiota for Immunomodulatory Organisms. Cell 2017; 168l, 928–943 e911.
33. Gomez de Aguero, M., Ganal-Vonarburg, S. C., Fuhrer, T., Rupp, S., Uchimura, Y., Li, H. *et al.* The maternal microbiota drives early postnatal innate immune development. Science 2016; 351l, 1296–1302.
34. Henrick, B. M., Rodriguez, L., Lakshmikanth, T., Pou, C., Henckel, E., Arzoomand, A. *et al.* Bifidobacteria-mediated immune system imprinting early in life. Cell 2021.
35. Roy, S. & Trinchieri, G. Microbiota: a key orchestrator of cancer therapy. Nat Rev Cancer 2017; 17l, 271–285.
36. Li, Y., Kundu, P., Seow, S. W., de Matos, C. T., Aronsson, L., Chin, K. C. *et al.* Gut microbiota accelerate tumor growth via c-jun and STAT3 phosphorylation in APCMin/+ mice. *Carcinogenesis* 2012; 33l, 1231–1238.
37. Lofgren, J. L., Whary, M. T., Ge, Z., Muthupalani, S., Taylor, N. S., Mobley, M. *et al.* Lack of commensal flora in Helicobacter pylori-infected INS-GAS mice reduces gastritis and delays intraepithelial neoplasia. Gastroenterology 2011; 140l, 210–220.
38. Chen, G. Y., Shaw, M. H., Redondo, G. & Nunez, G. The innate immune receptor Nod1 protects the intestine from inflammation-induced tumorigenesis. Cancer Res 2008; 68l, 10060–10067.
39. Dapito, D. H., Mencin, A., Gwak, G. Y., Pradere, J. P., Jang, M. K., Mederacke, I. *et al.* Promotion of hepatocellular carcinoma by the intestinal microbiota and TLR4. Cancer Cell 2012; 21l, 504–516.
40. Sivan, A., Corrales, L., Hubert, N., Williams, J. B., Aquino-Michaels, K., Earley, Z. M. *et al.* Commensal Bifidobacterium promotes antitumor immunity and facilitates anti-PD-L1 efficacy. Science 2015; 350l, 1084–1089.
41. Gopalakrishnan, V., Spencer, C. N., Nezi, L., Reuben, A., Andrews, M. C., Karpinets, T. V. *et al.* Gut microbiome modulates response to anti-PD-1 immunotherapy in melanoma patients. Science 2018; 359l, 97–103.

42. Sabus, A., Merrow, M., Heiden, A., Boster, J., Koo, J. & Franklin, A. R. K. Fecal Microbiota Transplantation for Treatment of Severe Clostridioides difficile Colitis in a Pediatric Patient With Non-Hodgkin Lymphoma. J Pediatr Hematol Oncol 2020.
43. Viaud, S., Saccheri, F., Mignot, G., Yamazaki, T., Daillere, R., Hannani, D. *et al.* The intestinal microbiota modulates the anticancer immune effects of cyclophosphamide. Science 2013; 342l, 971–976.
44. Routy, B., Le Chatelier, E., Derosa, L., Duong, C. P. M., Alou, M. T., Daillere, R. *et al.* Gut microbiome influences efficacy of PD-1-based immunotherapy against epithelial tumors. Science 2018; 359l, 91–97.
45. Yu, L. X. & Schwabe, R. F. The gut microbiome and liver cancer: mechanisms and clinical translation. Nat Rev Gastroenterol Hepatol 2017; 14l, 527–539.
46. Zhou, A., Tang, L., Zeng, S., Lei, Y., Yang, S. & Tang, B. Gut microbiota: A new piece in understanding hepatocarcinogenesis. Cancer Lett 2020; 474l, 15–22.
47. Ren, Z., Li, A., Jiang, J., Zhou, L., Yu, Z., Lu, H. *et al.* Gut microbiome analysis as a tool towards targeted non-invasive biomarkers for early hepatocellular carcinoma. Gut 2019; 68l, 1014–1023.
48. Ni, J., Huang, R., Zhou, H., Xu, X., Li, Y., Cao, P. *et al.* Analysis of the Relationship Between the Degree of Dysbiosis in Gut Microbiota and Prognosis at Different Stages of Primary Hepatocellular Carcinoma. *Front Microbiol* 2019; 10l, 1458.
49. Yuan, L., Hensley, C., Mahsoub, H. M., Ramesh, A. K. & Zhou, P. Microbiota in viral infection and disease in humans and farm animals. Prog Mol Biol Transl Sci 2020; 171l, 15–60.
50. Jiao, Y., Wu, L., Huntington, N. D. & Zhang, X. Crosstalk Between Gut Microbiota and Innate Immunity and Its Implication in Autoimmune Diseases. *Front Immunol* 2020; 11l, 282.
51. Helmink, B. A., Khan, M. A. W., Hermann, A., Gopalakrishnan, V. & Wargo, J. A. The microbiome, cancer, and cancer therapy. Nat Med 2019; 25l, 377–388.
52. Feng, Q., Chen, W. D. & Wang, Y. D. Gut Microbiota: An Integral Moderator in Health and Disease. *Front Microbiol* 2018; 9l, 151.
53. Iida, N., Dzutsev, A., Stewart, C. A., Smith, L., Bouladoux, N., Weingarten, R. A. *et al.* Commensal bacteria control cancer response to therapy by modulating the tumor microenvironment. Science 2013; 342l, 967–970.
54. Marigo, I., Zilio, S., Desantis, G., Mlecnik, B., Agnellini, A. H. R., Ugel, S. *et al.* T Cell Cancer Therapy Requires CD40-CD40L Activation of Tumor Necrosis Factor and Inducible Nitric-Oxide-Synthase-Producing Dendritic Cells. Cancer Cell 2016; 30l, 377–390.
55. Serbina, N. V., Salazar-Mather, T. P., Biron, C. A., Kuziel, W. A. & Pamer, E. G. TNF/iNOS-producing dendritic cells mediate innate immune defense against bacterial infection. Immunity 2003; 19l, 59–70.
56. Liu, F. D., Kenngott, E. E., Schroter, M. F., Kuhl, A., Jennrich, S., Watzlawick, R. *et al.* Timed action of IL-27 protects from immunopathology while preserving defense in influenza. PLoS Pathog 2014; 10l, e1004110.

57. Holscher, C., Holscher, A., Ruckerl, D., Yoshimoto, T., Yoshida, H., Mak, T. *et al.* The IL-27 receptor chain WSX-1 differentially regulates antibacterial immunity and survival during experimental tuberculosis. J Immunol 2005; 174l, 3534–3544.
58. Kao, J. T., Lai, H. C., Tsai, S. M., Lin, P. C., Chuang, P. H., Yu, C. J. *et al.* Rather than interleukin-27, interleukin-6 expresses positive correlation with liver severity in naive hepatitis B infection patients. Liver Int 2012; 32l, 928–936.
59. Cao, Y., Zhang, R., Zhang, W., Zhu, C., Yu, Y., Song, Y. *et al.* IL-27, a cytokine, and IFN-lambda1, a type III IFN, are coordinated to regulate virus replication through type I IFN. J Immunol 2014; 192l, 691–703.
60. Zhu, C., Zhang, R., Liu, L., Rasool, S. T., Mu, Y., Sun, W. *et al.* Hepatitis B virus enhances interleukin-27 expression both in vivo and in vitro. Clin Immunol 2009; 131l, 92–97.
61. Levrero, M. & Zucman-Rossi, J. Mechanisms of HBV-induced hepatocellular carcinoma. J Hepatol 2016; 64l, S84-S101.
62. Yuan, J. M., Wang, Y., Wang, R., Luu, H. N., Adams-Haduch, J., Koh, W. P. *et al.* Serum IL27 in Relation to Risk of Hepatocellular Carcinoma in Two Nested Case-Control Studies. Cancer Epidemiol Biomarkers Prev 2020.
63. Owaki, T., Asakawa, M., Morishima, N., Hata, K., Fukai, F., Matsui, M. *et al.* A role for IL-27 in early regulation of Th1 differentiation. J Immunol 2005; 175l, 2191–2200.
64. Huang, Z., Zak, J., Pratumchai, I., Shaabani, N., Vartabedian, V. F., Nguyen, N. *et al.* IL-27 promotes the expansion of self-renewing CD8(+) T cells in persistent viral infection. J Exp Med 2019; 216l, 1791–1808.
65. Brender, C., Tannahill, G. M., Jenkins, B. J., Fletcher, J., Columbus, R., Saris, C. J. *et al.* Suppressor of cytokine signaling 3 regulates CD8 T-cell proliferation by inhibition of interleukins 6 and 27. *Blood* 2007; 110l, 2528–2536.
66. Horlad, H., Ma, C., Yano, H., Pan, C., Ohnishi, K., Fujiwara, Y. *et al.* An IL-27/Stat3 axis induces expression of programmed cell death 1 ligands (PD-L1/2) on infiltrating macrophages in lymphoma. Cancer Sci 2016; 107l, 1696–1704.
67. Sha, S., Ni, L., Stefil, M., Dixon, M. & Mouraviev, V. The human gastrointestinal microbiota and prostate cancer development and treatment. Investig Clin Urol 2020; 61l, S43-S50.
68. Riquelme, E., Zhang, Y., Zhang, L., Montiel, M., Zoltan, M., Dong, W. *et al.* Tumor Microbiome Diversity and Composition Influence Pancreatic Cancer Outcomes. Cell 2019; 178l, 795–806 e712.
69. Taur, Y., Coyte, K., Schluter, J., Robilotti, E., Figueroa, C., Gjonbalaj, M. *et al.* Reconstitution of the gut microbiota of antibiotic-treated patients by autologous fecal microbiota transplant. Sci Transl Med 2018; 10l.
70. Patel, T., Bhattacharya, P. & Das, S. Gut microbiota: an Indicator to Gastrointestinal Tract Diseases. J Gastrointest Cancer 2016; 47l, 232–238.
71. Li, Y., Elmen, L., Segota, I., Xian, Y., Tinoco, R., Feng, Y. *et al.* Prebiotic-Induced Anti-tumor Immunity Attenuates Tumor Growth. Cell Rep 2020; 30l, 1753–1766 e1756.

72. Mager, L. F., Burkhard, R., Pett, N., Cooke, N. C. A., Brown, K., Ramay, H. *et al.* Microbiome-derived inosine modulates response to checkpoint inhibitor immunotherapy. Science 2020; 369l, 1481–1489.
73. Leon, B., Lopez-Bravo, M. & Ardavin, C. Monocyte-derived dendritic cells formed at the infection site control the induction of protective T helper 1 responses against Leishmania. Immunity 2007; 26l, 519–531.
74. Aldridge, J. R., Jr., Moseley, C. E., Boltz, D. A., Negovetich, N. J., Reynolds, C., Franks, J. *et al.* TNF/iNOS-producing dendritic cells are the necessary evil of lethal influenza virus infection. Proc Natl Acad Sci U S A 2009; 106l, 5306–5311.
75. Kuhn, S., Yang, J. & Ronchese, F. Monocyte-Derived Dendritic Cells Are Essential for CD8(+) T Cell Activation and Antitumor Responses After Local Immunotherapy. *Front Immunol* 2015; 6l, 584.

Figures

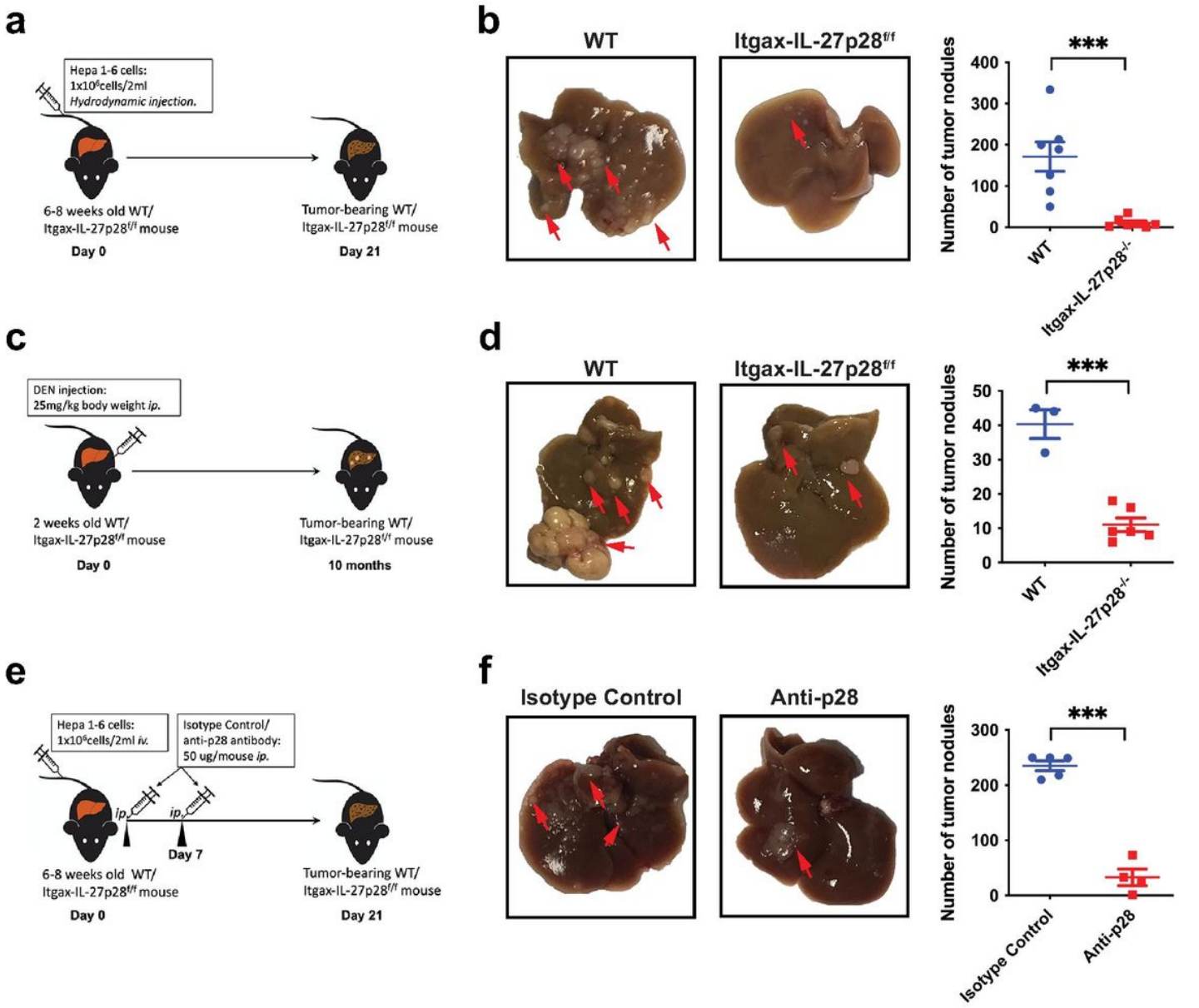

Figure 1

Figure 1

DC-derived IL-27 promoted tumor development in murine HCC models. (a-b) Hepa1-6 cells were injected into the recipient mice (WT or Itgax-IL-27p28$^{f/f}$ mice) by hydrodynamic injection (1×10^6 cells/2ml/mouse, n=6 mice per group) (a). On day 21, the tumor-bearing mice were euthanized and the number of tumor nudes in the liver was counted (b). (c-d) WT or Itgax-IL-27p28$^{f/f}$ mice (3–6 mice/group) were injected intraperitoneally with 25 mg/kg DEN on day 14 after birth (c). The number of tumor nodules in the liver was counted at the end of the ten months (d). (e-f) Hepa1-6 cells were injected into the recipient WT mice by hydrodynamic injection (1×10^6 cells/2ml/mouse, n≥ 4 mice per group). Anti-p28 neutralizing antibody

(50ug/mouse, *ip.*) was injected into recipient mice on day 0 and day7 (e). On day 21, the tumor-bearing mice were euthanized and the number of tumor nudes in the liver was counted (f). The representative of tumor morphology (left panels) and the numbers of tumor nodules (right panels) are shown. The data shown are mean ± SEM. Data are the representative of at least two independent experiments. Statistical analysis was performed using Two-tail unpaired student's t-test. ***p <0.001.

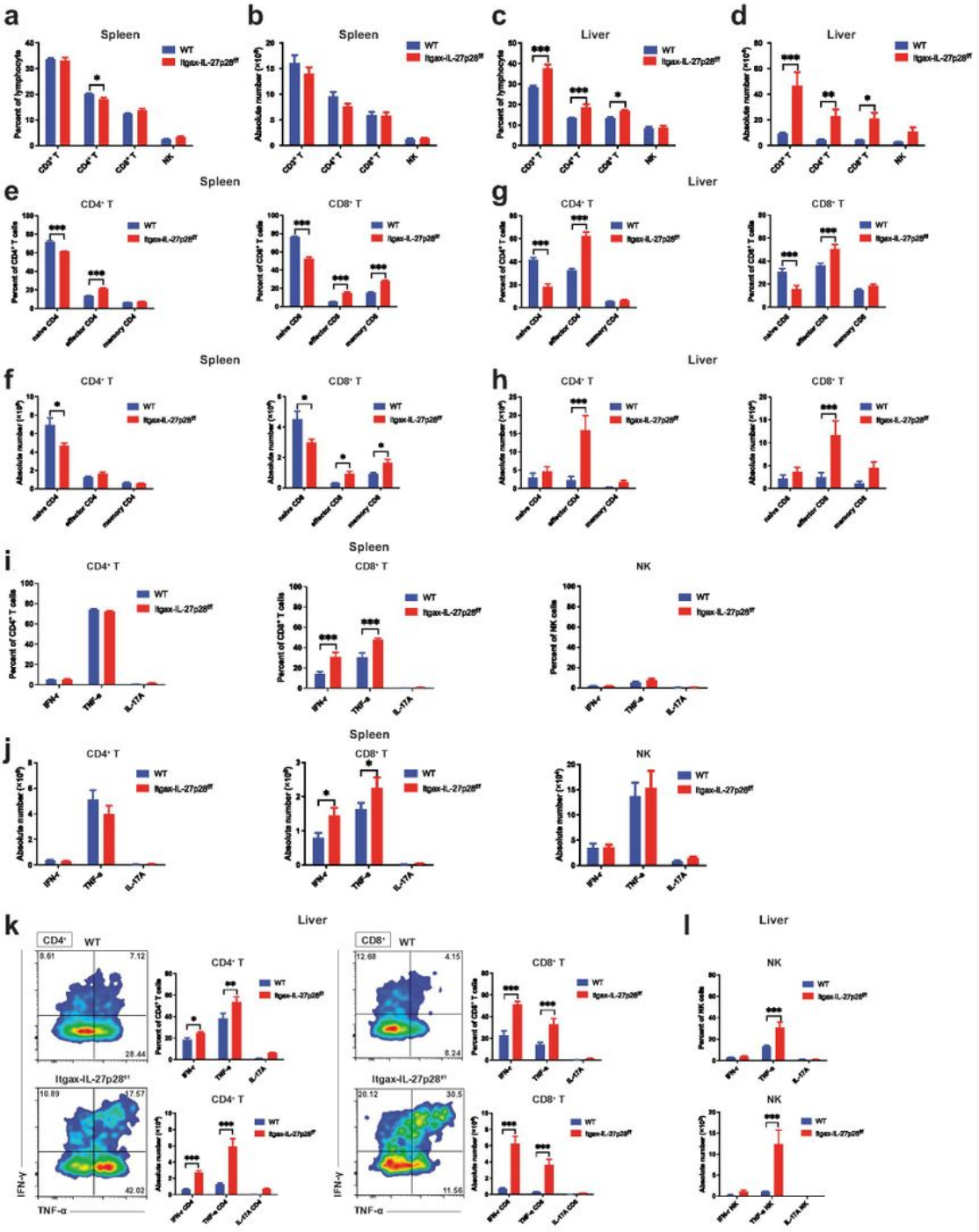

Figure 2

Figure 2

DC-derived IL-27 inhibited T cell activation in the tumor microenvironment. Hepa1-6 cells were injected into the recipient mice (WT or Itgax-IL-27p28$^{f/f}$ mice) by hydrodynamic injection (1×10^6 cells/2ml/mouse, n ≥ 5 mice per group). On day 21, the tumor-bearing mice were euthanized, and the lymphocytes were isolated from the spleen and tumor-bearing liver. (a-b) The percentages (a) and absolute numbers (b) of CD3$^+$T, CD4$^+$T, CD8$^+$T and NK cells in the tumor-bearing spleen from WT or Itgax-IL-27p28$^{f/f}$ mice. (c-d) The percentages (c) and absolute numbers (d) of CD3$^+$T, CD4$^+$T, CD8$^+$T and NK cells in the tumor-bearing liver of WT or Itgax-IL-27p28$^{f/f}$ mice. (e-f) The percentages (e) and absolute numbers (f) of naïve, effector and memory CD4$^+$T (left) or CD8$^+$T (right) cells in the spleen from tumor-bearing WT or Itgax-IL-27p28$^{f/f}$ mice. (g-h) The percentages (g) and absolute numbers (h) of naïve, effector and memory CD4$^+$T (left) or CD8$^+$T (right) cells in the liver from tumor-bearing WT or Itgax-IL-27p28$^{f/f}$ mice. (i-j) The percentages (i) and absolute numbers (j) of IFN-γ, TNF-α or IL-17a producing CD4$^+$T (left), CD8$^+$T (middle) or NK (right) cells in the tumor-bearing spleen of WT or Itgax-IL-27p28$^{f/f}$ mice. (k) The percentages (up) and absolute numbers (bottom) of IFN-γ, TNF-α or IL-17a producing CD4$^+$T (left) or CD8$^+$T (right) cells in the tumor-bearing liver of WT or Itgax-IL-27p28$^{f/f}$ mice. The expression of IFN-γ or TNF-α was shown as density plots. (l) The percentages (up) and absolute numbers (bottom) of IFN-γ, TNF-α or IL-17a producing NK cells in the tumor-bearing liver of WT or Itgax-IL-27p28$^{f/f}$ mice.

The data shown are mean ± SEM. Data are the representative of at least two independent experiments. Statistical analysis was performed using Two-tail unpaired student's t-test. *p < 0.05, **p < 0.01, ***p <0.001.

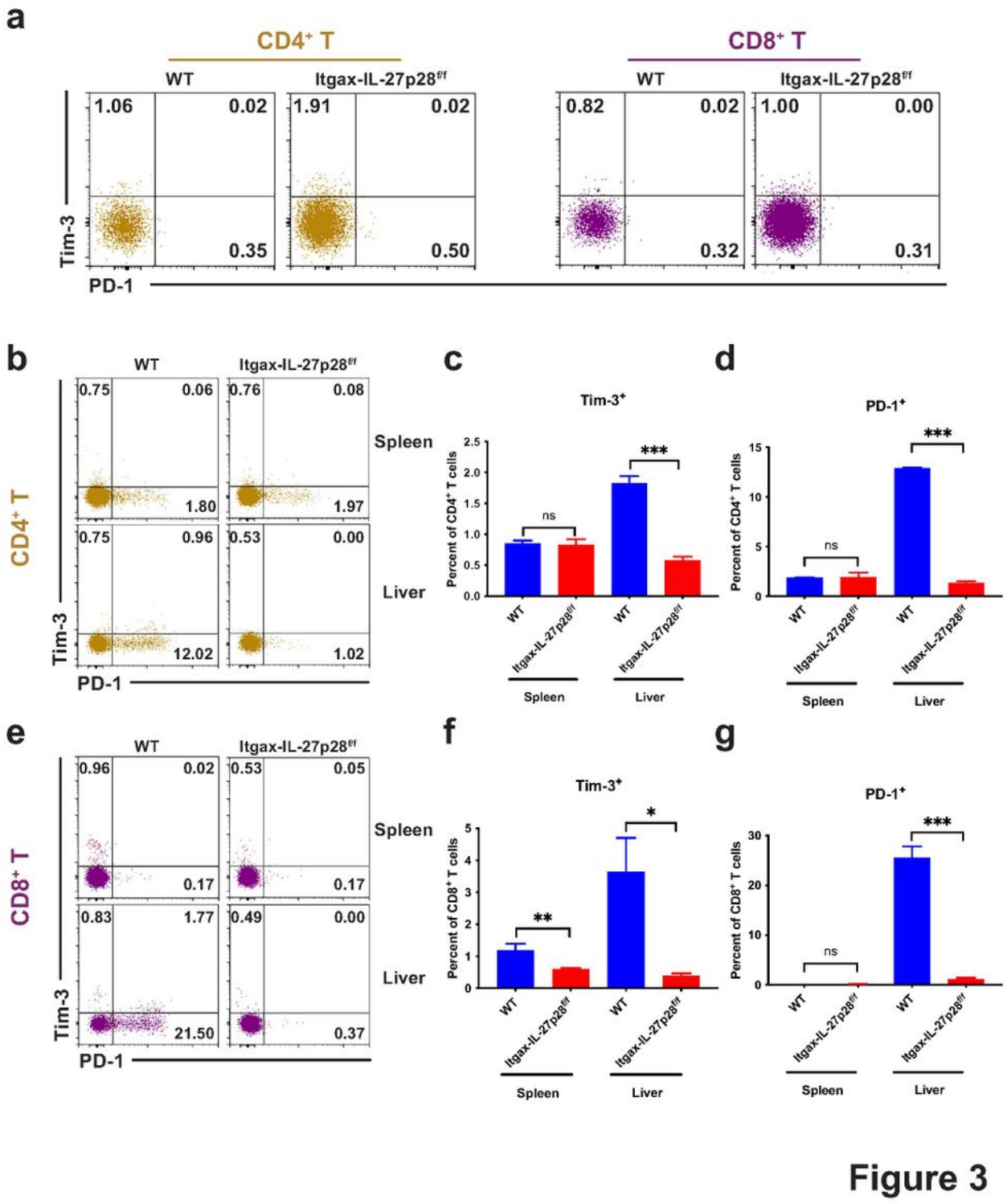

Figure 3

Figure 3

DC-derived IL-27 promoted the expression of inhibitory receptors on both CD4$^+$ and CD8$^+$ T cells in tumor-bearing mice. (a) The expressions of Tim-3 and PD-1 on CD4$^+$T and CD8$^+$T cells from the liver of naïve WT or Itgax-IL-27p28$^{f/f}$ mice. (b-d) The expressions of Tim-3 (c) and PD-1 (d) on CD4$^+$T cells in spleen or liver from the tumor-bearing WT or Itgax-IL-27p28$^{f/f}$ mice. (e-g) The expressions of Tim-3 (f) and PD-1 (g) on CD8$^+$T cells in spleen or liver from the tumor-bearing WT or Itgax-IL-27p28$^{f/f}$ mice. The data shown are

mean ± SEM. Data are the representative of at least two independent experiments. Statistical analysis was performed using one-way ANOVA followed by Dunnett's multiple comparisons test. *p < 0.05, **p < 0.01, ***p <0.001.

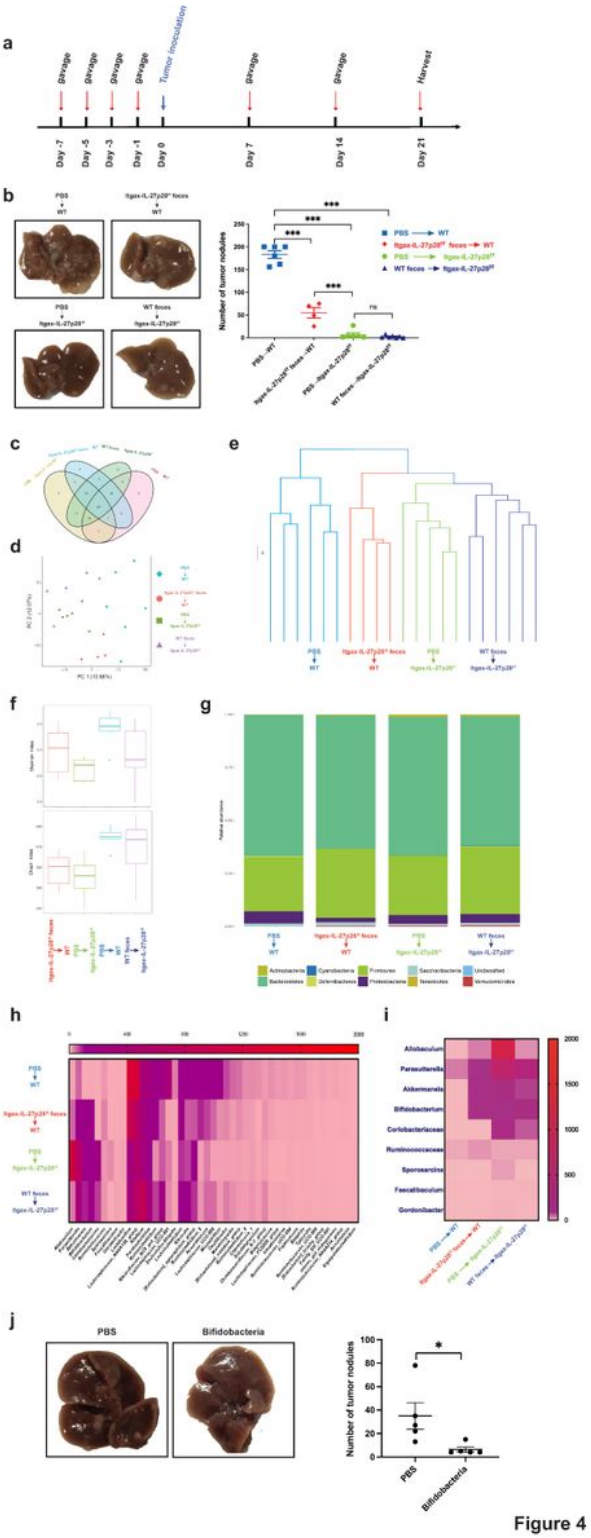

Figure 4

Figure 4

DC-derived IL-27 affected tumor development through modulating gut microbiota. (a) Experimental design: we harvested the feces of WT or Itgax-IL-27p28$^{f/f}$ mice and dissolved with PBS, then gavage the host mice on day -7 to day 0 (once every 2 days) before tumor inoculation. On day 0, mice were hydrodynamically injected with hepa1-6 cells (1×10^6 cells/2ml/mouse, $n \geq 5$ mice per group). After tumor injection, the host mice received fecal transplant once a week. On day 21, the number of tumor nodes was counted. 16s RNA sequence analysis was performed with feces collected on day 21. (b) The tumor nodes in the liver were counted on day 21. Data shown are representative of tumor morphology (top panel) and the numbers of tumor nodules shown as mean ± SEM (bottom panel). (c-i) The microbiota collected from mice received PBS, feces from WT or Itgax-IL-27p28$^{f/f}$ mice by gavage were sequenced and analyzed. Venn diagram (c), PCA (d), and UPGMA-TREE (e) were shown from indicated groups. Each dot or line represents one sample in the group (4 to 6 mice per group.). Shannon index and Chao index (f) displayed the diversity and richness of microbiota in each group. Relate abundance at phylum level and genus level were show as community (g) and heatmap (h & i). Columns in heatmap denote bacterial OTUs; rows denote groups by different treatment. The up-regulated genus of bacteria in Itgax-IL-27p28$^{f/f}$ mice compare with WT mice were presented (i). (j) We transfer bifidobacterial cocktail or PBS to WT mice by gavage on day -7 to day 0 (once every 2 days). On day 0, mice were hydrodynamically injected with hepa1-6 cells (1×10^6 cells/2ml/mouse, $n \geq 5$ mice per group). After tumor injection, the host mice received fecal transplant once a week. The tumor nodes in the liver were counted on day 21. Data shown are representative of tumor morphology (top panel) and the numbers of tumor nodules shown as mean ± SEM (bottom panel).

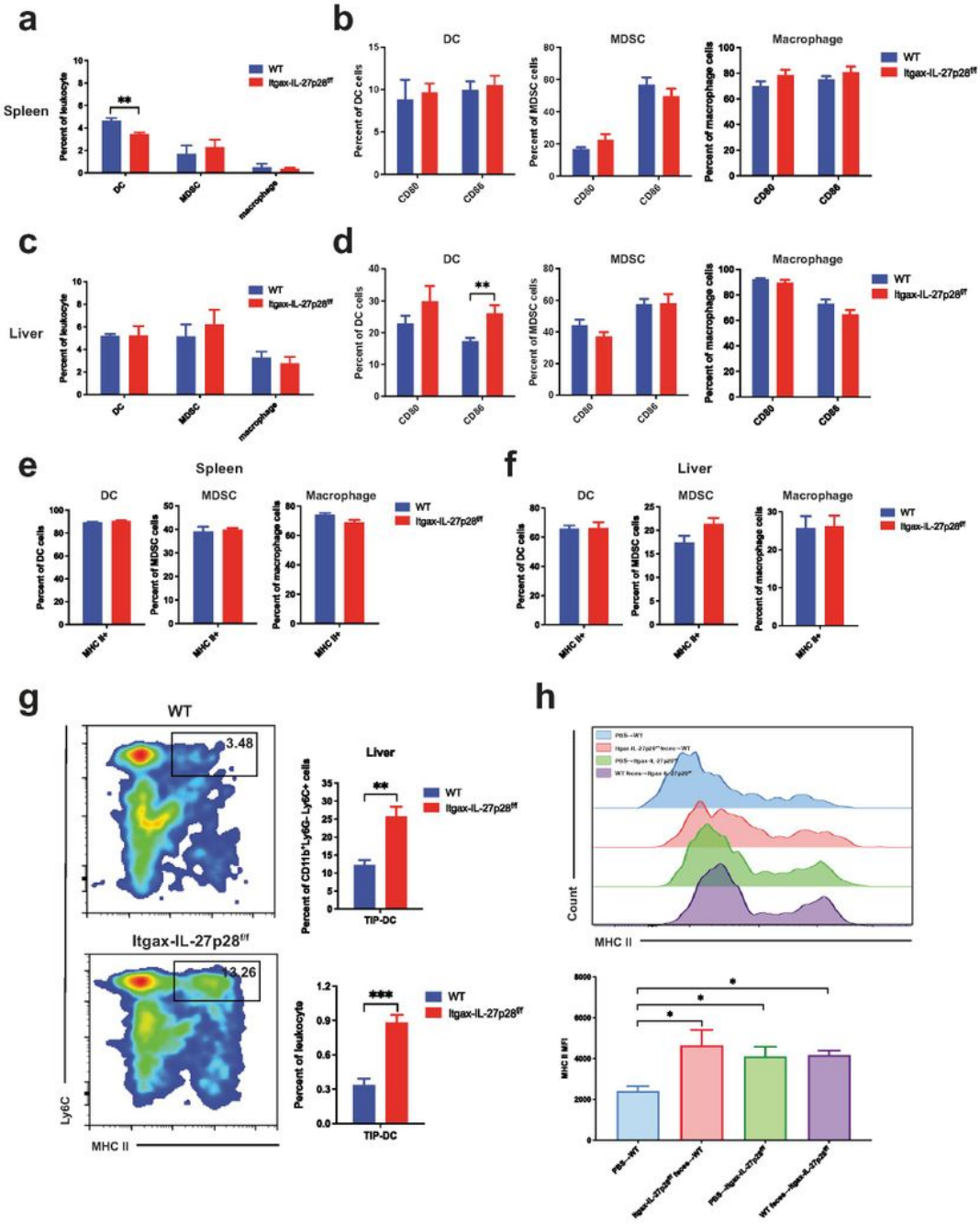

Figure 5

Figure 5

Ly6C^{+}MHCII^{+} (TIP)-DCs could be modulated by gut microbiota in the absence of DC-derived IL-27. Hepa1-6 cells were injected into the recipient mice (WT or Itgax-IL-27p28$^{f/f}$ mice) by hydrodynamic injection (1×10^{6} cells/2ml/mouse, n ≥ 5 mice per group). On day 21, the tumor-bearing mice were euthanized, and the leukocyte were isolated from the spleen and tumor-bearing liver for flow analysis. (a) The percentages

of DC, MDSC and macrophages in the spleen from WT or Itgax-IL-27p28$^{f/f}$ mice. (b) The expression of CD80 or CD86 on DC (left), MDSC (middle), or macrophage (right) in the spleen from WT or Itgax-IL-27p28$^{f/f}$ mice. (c) The percentages of DC, MDSC and macrophages in the liver from WT or Itgax-IL-27p28$^{f/f}$ mice. (d) The expression of CD80 or CD86 on DC (left), MDSC (middle), or macrophage (right) in the liver from WT or Itgax-IL-27p28$^{f/f}$ mice. (e-f) The expression of MHC II on DC (left), MDSC (middle), or macrophage (right) in the spleen (e) or liver (f) from WT or Itgax-IL-27p28$^{f/f}$ mice. (g) The gating strategy (left), percentage of CD11b^{+}Ly6G^{-}Ly6C^{+}MHC-II^{+} cells (TIP-DC) out of CD11b^{+}Ly6G^{-}Ly6C^{+} monocyte (right up) or total leukocyte (right bottom) in the tumor-bearing liver from WT or Itgax-IL-27p28$^{f/f}$ mice. (h) The MHI II expression on TIP-DC from tumor-bearing live of mice received PBS, feces from WT or Itgax-IL-27p28$^{f/f}$ mice by gavage. Data shown are mean ± SEM. Data are representative of at least two independent experiments. Two-tail unpaired student's t-test was used for statistical analysis. **p< 0.01, ***p<0.001.

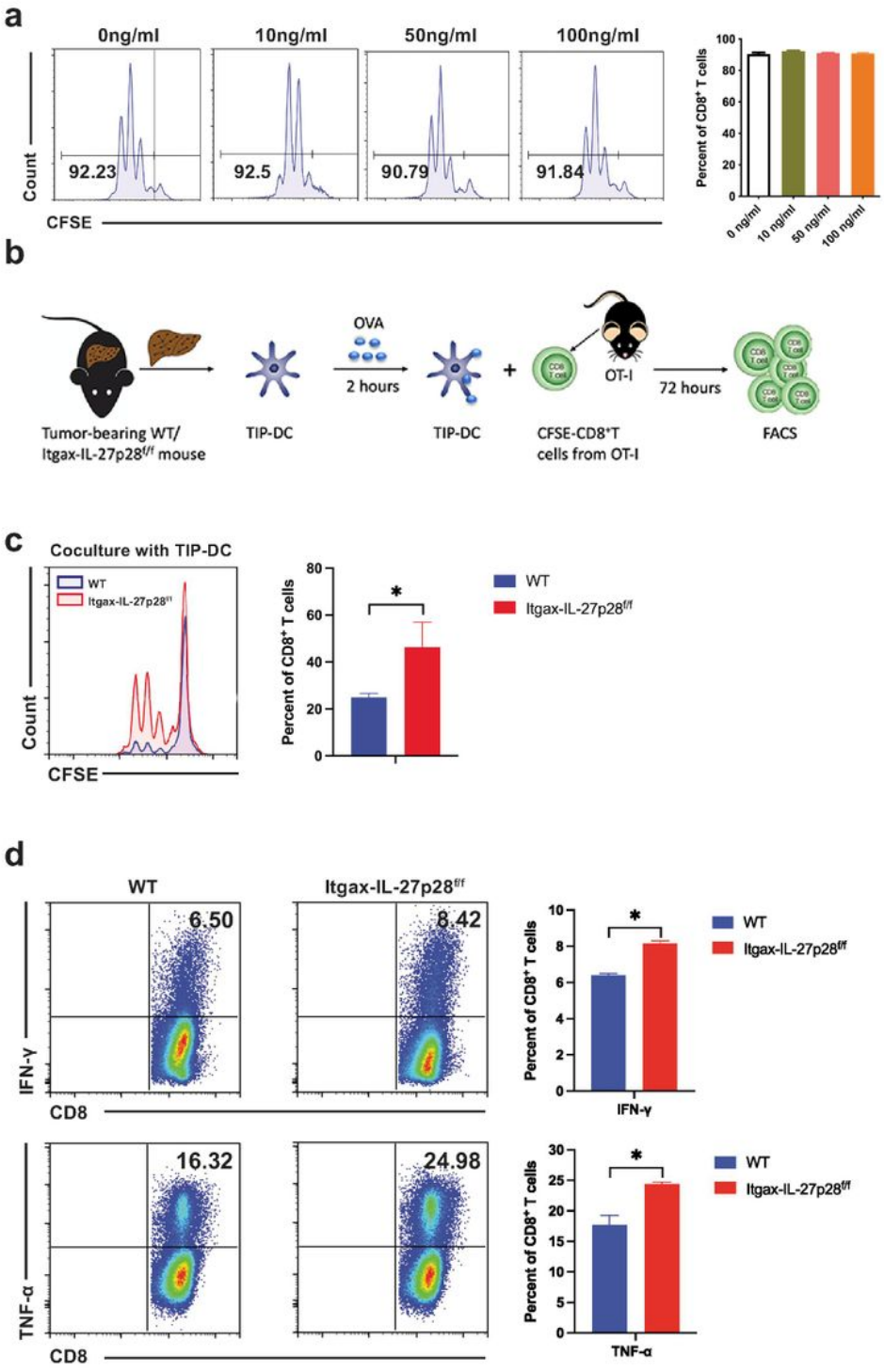

Figure 6

Figure 6

TIP-DCs are more potent in activating T cells in the absence of DC-derived IL-27. (a) $CD8^+$T cells from C57BL/6 OT-1 mouse were labelled with CFSE and stimulated with anti-mouse CD3 (5ug/ml) and anti-mouse CD28 (2.5ug/ml) in the presence of various concentrations of rmIL-27 as indicated. 3 days later, the proliferation of $CD8^+$T cells was analyzed by flow cytometry. (b) Experimental design: $CD8^+$ T cells isolated from OT-1 mice were co-cultured with TIP-DCs from tumor-bearing WT or Itgax-IL-27p28$^{f/f}$ mice

pulsed with OVA for three days. (c) The proliferation of $CD8^+$T cells analyzed by flow cytometry after co-culture with OVA pulsed TIP-DCs from WT or Itgax-IL-$27p28^{f/f}$ tumor-bearing liver. (d) The IFN-γ (top) and TNF-α (bottom) productions in $CD8^+$T cells after co-cultured with OVA pulsed TIP-DCs from WT or Itgax-IL-$27p28^{f/f}$ tumor-bearing liver by flow cytometry. The expression of IFN-γ or TNF-α were show as dot plot (left). Data shown are mean ± SEM. Data are representative of at least two independent experiments. Two-tail unpaired student's t-test (a-c) or one-way ANOVA followed by Dunnett's multiple comparisons test (d) was used for statistical analysis. * $p < 0.05$, **$p< 0.01$, ***$p<0.001$.

Supplementary Files

This is a list of supplementary files associated with this preprint. Click to download.

- IL27paperMicrobiomeSupplementaryData.docx